Closed-Loop Transition Induced by Homopolymers

Eunhye Kim,[†] Hyungju Ahn,[†] Du Yeol Ryu,*[,†] Wonchul Joo,[‡] Jin Kon Kim,*[,‡] Jueun Jung,[§] and Taihyun Chang[§]

Department of Chemical Engineering, Yonsei University, Seoul 120-749, Korea, National Creative Research Initiative Center for Block Copolymer Self-Assembly, Department of Chemical Engineering and Polymer Research Institute, Pohang University of Science and Technology, Pohang, Gyeongpuk 790-784, Korea, and Department of Chemistry and Polymer Research Institute, Pohang University of Science and Technology, Gyeongpuk 790-784, Korea

Received July 8, 2008; Revised Manuscript Received September 16, 2008

ABSTRACT: The phase behavior for the binary mixtures of a polystyrene-*block*-poly(*n*-pentyl methacrylate) (PS-*b*-P*n*PMA) and homopolystyrenes (PS) with various molecular weights was investigated by depolarized light scattering and small-angle X-ray scattering (SAXS) as a function of PS amount. A homopolymer-free PS-*b*-P*n*PMA, prepared by a high performance liquid chromatography (HPLC) technique, showed the entirely disordered (or homogeneous) state within experimental temperature range from the glass transition temperature (T_g) to the thermal degradation temperature (T_d). By adding PS to this PS-*b*-P*n*PMA, the closed-loop phase behavior was observed for the binary mixtures where no macrophase separation occurred. With increasing molecular weight (chain length) of PS, the ordered range of the closed-loop extended remarkably and a critical amount of PS increased, resulting in the conservation of only lamellar morphology up to the overall PS volume fraction (f_{PS}) of 0.70 for a PS, having a chain length ratio (α) of 2 with respect to the PS chain length of PS-*b*-P*n*PMA.

Introduction

The phase behaviors of the binary mixtures composed of a block copolymer (BCP) and homopolymer have been of great concern since they allow various ordered structures or disordered state effectively by the relative composition and the degree of miscibility between two.[1−33] The effect of composition and molecular weight (or chain length ratio; α) of homopolymer to the corresponding block component on the phase behavior has been one of the primary interests for the mixtures of BCP/homopolymer.[2−6,8,9,12−17,19−25,27−30,32] In the case of low molecular weight of homopolymers ($\alpha \ll 1$), they generally tend to be solubilized homogeneously into one or both of the microdomains of BCP. With increasing molecular weight of homopolymers, they are solubilized into near the center of the selective microdomain. When a high molecular weight homopolymer ($\alpha \gg 1$) is added, the macrophase separation may take place, therefore the miscibility between the homopolymer and confined chain in the BCP involves the loss of combinatorial entropy.[21]

Many research groups investigated the phase behavior for the mixtures of BCP/homopolymer having an order-to-disorder transition (ODT) experimentally and theoretically, which can be explained by the entropy, the segmental interactions, and the microphase transform induced by the addition of homopolymer.[1−31] For the mixtures of BCP/homopolymer having a lower disorder-to-order transition (LDOT) upon heating, Kim et al. produced the phase diagram for the mixtures of polystyrene-*block*-poly(*n*-butyl methacrylate) (PS-*b*-P*n*BMA) and the corresponding homopolymers and compared with the compressible random phase approximation prediction, where LDOT was altered by homopolymers.[32] This LDOT can be rather described by the difference of compressibility and the weak specific interactions upon heating, which were found in polystyrene-*block*-poly(ethyl methacrylate) (PS-*b*-PEMA), and polystyrene-*block*-poly(*n*-propyl methacrylate) (PS-*b*-P*n*PrMA).[34,35]

Recently, a closed-loop phase transition, having both transition temperatures of LODT and upper order−disorder transition (UODT) upon heating, was observed in the weakly interacting system such as polystyrene-*block*-poly(*n*-pentyl methacrylate) (PS-*b*-P*n*PMA)[36−42] This phase behavior is caused by the balance between the weak intermolecular interaction and the entropy by disparity in the compressibility as well as by the chain conformation over the narrow range of molecular weight.

Upon heating, the entropic volume fluctuations by the compressibility difference under weak specific interactions cause the microphase separation at a lower temperature, whereas at higher temperature combinatorial entropy on mixing is more predominant. These two transitions are referred to as an LDOT and a UODT, respectively.[43]

It was recently reported that the closed-loop phase transition of PS-*b*-P*n*PMA is sensitive to average molecular weight, chemical composition and compositional broadness by which the delicate energetic variation is brought about.[44] Theoretically, it was reported by Cho that from the Hartree (fluctuation correction) analysis for compressible diblock copolymers, an effective Flory-type interaction parameter carries not only the change in contact interactions but also compressibility difference between two block constituents, where infinite but small specific interaction plays a primary role on forming a closed-loop.[45]

In this study, the phase behavior for the binary mixtures of PS-*b*-P*n*PMA and PS homopolymers with various molecular weights was investigated in terms of transition temperatures. We found that a disordered (or homogeneous) state for homopolymer-free PS-*b*-P*n*PMA, prepared by a high performance liquid chromatography (HPLC) technique, can be transformed into the closed-loop phase transition in the mixtures with PS homopolymers at accessible temperatures range. To the best of our knowledge, this is the first report on the microphase separation induced by homopolymers from a disordered state of BCP, suggesting that closed-loop phase behavior is sensitive to the relative composition as well as the molecular weight of PS added.

* To whom correspondence should be addressed. E-mail: dyryu@yonsei.ac.kr (D.Y.R.); jkkim@postech.ac.kr (J.K.K).
[†] Department of Chemical Engineering, Yonsei University.
[‡] National Creative Research Initiative Center for Block Copolymer Self-Assembly, Department of Chemical Engineering and Polymer Research Institute, Pohang University of Science and Technology.
[§] Department of Chemistry and Polymer Research Institute, Pohang University of Science and Technology.

10.1021/ma801530f CCC: $40.75
Published on Web 11/26/2008

Table 1. Molecular Characteristics of a Block Copolymer and Homopolymers

specimen	description	M_n[a]	M_w/M_n[a]	f_{PS}[b]	state
PS-*b*-P*n*PMA	polystyrene-*block*-poly(*n*-pentyl methacrylate)	53 700	1.01	0.465	disordered
PS-06	PS homopolymer	6500	1.06	1.0	
PS-13	PS homopolymer	12 600	1.04	1.0	
PS-25	PS homopolymer	24 600	1.03	1.0	
PS-46	PS homopolymer	45 500	1.04	1.0	

[a] Weight- and number-average molecular weights (M_w and M_n) and polydispersity (M_w/M_n) were measured by size-exclusion chromatography with multiangle laser light scattering (SEC-MALLS). [b] Volume fraction of PS for PS*b*-P*n*PMA copolymer was measured by ^{1}H nuclear magnetic resonance (NMR) with mass densities of two components (1.05 and 1.03 g/ cm^3 for PS and P*n*PMA, respectively).

Experimental Section

A symmetric PS-*b*-P*n*PMA was synthesized by the sequential, anionic polymerization of styrene and *n*-pentyl methacrylate in tetrahydrofuran at −78 °C in the presence of LiCl (high purity, Aldrich) under purified argon using *sec*-butyllithium as an initiator. For the precise composition of the binary mixtures, PS-*b*-P*n*PMA was clearly purified by eliminating all PS homopolymers which was still left during anionic polymerization process. A high performance liquid chromatography (HPLC) system was used for the reversed phase liquid chromatography (RPLC) separation of the PS-*b*-P*n*PMA, where a C_{18} (octadecylsilane) column (70 × 22 mm I.D.) and CH_2Cl_2/CH_3CN eluent (62/38, v/v) were used as the stationary phase and the mobile phase at constant temperature of 34 °C, respectively.[44]

The absolute weight- and number-average molecular weights (M_w and M_n) and polydispersity (M_w/M_n) were measured by size-exclusion chromatography (SEC) with multiangle laser light scattering (MALLS) and PS volume fraction of homopolymer-free PS-*b*-P*n*PMA was determined to be 0.465 by ^{1}H nuclear magnetic resonance (^{1}H NMR) with mass densities of two components (1.05 and 1.03 g/cm^2 for PS and P*n*PMA, respectively). Four kinds of PS with $\alpha = 0.25$, 0.5, 1, and 2 were synthesized anionically and the molecular characteristics for PS-*b*-P*n*PMA and PS employed in this study are given in Table 1.

The binary mixtures of PS-*b*-P*n*PMA/PS were prepared by freeze-drying method with benzene as a cosolvent. For instance, a predetermined amount of PS-*b*-P*n*PMA and PS were dissolved in benzene (~8 wt % in solute) and the quenched solution was evaporated under vacuum for 24 h, followed by sequential annealing at $T = 110$ °C for 24 h to thermally equilibrate the sample and to remove the solvent completely. The transition temperatures for the samples were measured by the depolarized light scattering using a polarized beam from a He−Ne laser at a wavelength of 632.8 nm, where the intensity detected at photodiode through an A/D converter was recorded as a function of temperature at the heating rate of 0.5 °C /min from 110 to 300 °C under nitrogen flow.

Synchrotron small-angle X-ray scattering (SAXS) measurements were performed in 4C1 and 4C2 beamlines at the Pohang Light Source (PLS), Korea. The wavelength (λ) of the X-ray beam was 1.608Å, and the energy resolution ($\Delta\lambda/\lambda$) was 1.5×10^{-2}. A-2D CCD camera (Princeton Instruments Inc., SCX-TE/CCD-1242) was used to collect the scattered X-rays. Experimental conditions were set up in typical beam size of 1 × 1 mm^2, sample thickness of 1.5 mm, and sample-to-detector distance of 3 m. A homemade heating cell was used for temperature sweep experiment and all the experiments were carried out under the nitrogen flow in order to avoid thermal degradation of the polymer samples.

Results and Discussion

Figure 1 displays the chromatograms of the neat PS-*b*-P*n*PMA and homopolymer-free PS-*b*-P*n*PMA, in which the intensity was recorded by the absorbance at a wavelength of 260 nm as a function of elution time. The SEC chromatogram, as given in Figure 1a, shows a narrow and unimodal elution peak for two

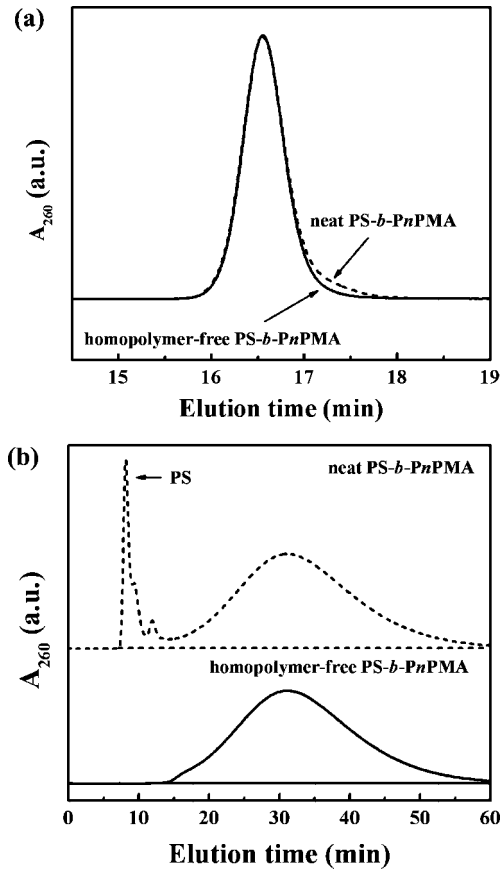

Figure 1. (a) SEC and (b) isothermal IC chromatograms for the neat PS-*b*-P*n*PMA (dashed lines) and homopolymer-free PS-*b*-P*n*PMA (solid lines), which were recorded by the absorbance at a wavelength of 260 nm. After IC separation, the elimination of uncoupled PS leads to a little decrease of PS volume fraction in PS-*b*-P*n*PMA from 0.50 to 0.465.

samples although the neat PS-*b*-P*n*PMA has a little tail at lower molecular weight regime (longer retention time), which is attributed to the uncoupled PS homopolymers during anionic block copolymerization process. This difference appears evidently in Figure 1b when the BCPs were subjected to isothermal interaction chromatography (IC) because of the effective separation by the differences in the interaction strength of the P*n*PMA chains with the stationary phase in this system.[44] A narrow peak detected at early elution time (dashed line before 11 min) corresponds to uncoupled PS homopolymers due to the undesired impurities such as water and oxygen,[46] thereby possibly affecting the phase behaviors of PS-*b*-P*n*PMA. Uncoupled PS homopolymers was subsequently removed from the neat PS-*b*-P*n*PMA in order to avoid possible arguments concerning the residual PS homopolymers in the mixtures of PS-*b*-P*n*PMA/PS, hereafter denoted to homopolymer-free PS-*b*-P*n*PMA or PS-*b*-P*n*PMA. It is seen in Figure 1b that after IC separation PS homopolymers were successfully eliminated, leading to a little decrease of volume fraction of PS in PS-*b*-P*n*PMA from 0.50 to 0.465.

SAXS profiles for the homopolymer-free PS-*b*-P*n*PMA measured at various temperatures from 110 to 245 °C during heating process are shown in Figure 2a as a function of scattering vector (q), where $q = (4\pi/\lambda)(\sin\theta)$, 2θ and λ are the scattering angle and wavelength, respectively. At low temperatures, as taken at 110 °C, a weak and broad scattering maximum was observed due to the correlation hole scattering of BCP in disordered state.[47] As temperature increases this diffuse maximum persists up to 245 °C although the intensity increases gradually, confirming the entirely disordered state of

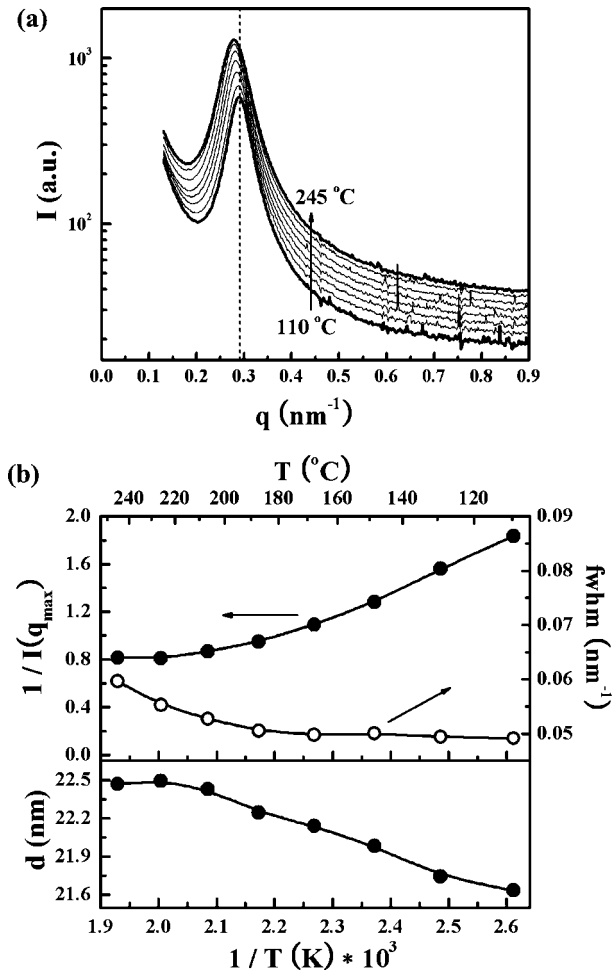

Figure 2. (a) SAXS profiles for homopolymer-free PS-*b*-P*n*PMA measured at various temperatures from 110 to 245 °C during heating process. (b) Temperature dependence of the inverse of the maximum intensity ($1/I(q_{max})$), full-width at half-maximum (fwhm), and *d*-spacing (d) by $d = 2\pi/q_{max}$. A weak and broad maximum due to the correlation hole scattering indicates the entirely disordered state of PS-*b*-P*n*PMA within the experimental temperature range.

PS-*b*-P*n*PMA within the experimental temperature range. The inverse of the maximum intensity ($1/I(q_{max})$), full-width at half-maximum (fwhm) and *d*-spacing (*d*) taken by $d = 2\pi/q_{max}$ are plotted in Figure 2b as a function of inverse temperature ($1/K$), which are derived from the SAXS profiles. With increasing temperature, only a gradual decrease of $1/I(q_{max})$, a little increase of fwhm, and the increase of *d*-spacing without any discontinuity indicate that PS-*b*-P*n*PMA hence remains disordered. Different from a ODT phase showing the opposite tendency in $1/I(q_{max})$ and *d*-spacing, these behaviors have turned out to be a LDOT or potentially closed-loop phase having a minimum in $1/I(q_{max})$ at higher molecular weight of this system, which are consistent with the previous results.[36,37] In addition, it is not surprising that this molecular weight of 53 700 g/mol ($f_{PS} = 0.465$) for PS-*b*-P*n*PMA exhibited a disordered state in comparison to 50 000 g/mol ($f_{PS} = 0.50$) having a closed-loop in the prior study,[36] because it has been previously found that the closed-loop phase transition of PS-*b*-P*n*PMA is very sensitive to average chain size (or average molecular weight), average chemical composition and compositional broadness presumably due to the delicate energetic variations between two block components in the PS-*b*-P*n*PMA.[44]

Figure 3 shows the depolarized light scattering intensity for the mixtures of PS-*b*-P*n*PMA/PS-13 by varying the amount of PS-13 (or weight fraction of PS-13; $W_{PS\text{-}13}$), having $\alpha = 0.5$ with respect to the PS chain length of PS-*b*-P*n*PMA. Over the entire temperature range where all the data were taken at 0.1 °C intervals from 110 to 230 °C at a heating rate of 0.5 °C/min, intensity for PS-*b*-P*n*PMA with no PS did not show any scattering intensity due to the optical isotropy of the disordered state, which is consistent with SAXS results in Figure 2. When small amount of PS-13 was blended at $W_{PS\text{-}13} = 0.04$ (corresponding to the overall PS volume fraction; $f_{PS} = 0.49$), the intensity begins to increase at 150 °C with increasing temperature, reaches a maximum, and followed by a sharp decrease at nearly 182 °C to zero, holding the same with further increasing temperature up to 230 °C. These increase and decrease in the depolarized light scattering intensity coincide with a LDOT and a UODT, respectively, indicating a closed-loop phase transition. The ordered range, characterized by the gap between two transition temperatures of closed-loop, are maximized at $W_{PS\text{-}13} = 0.11$ of the mixtures, having a LDOT at 118 °C and a UODT at 211 °C. At $W_{PS\text{-}13} = 0.17$, however, LDOT increased and UODT decreased compared to those two transitions at $W_{PS\text{-}13} = 0.11$, and the intensity was not detected again at $W_{PS\text{-}13} = 0.23$, indicating a disordered state for this mixture. Such a phase change, from disordered through closed-loop to disordered state, with increasing the amount of PS-13 suggests that the simple blending with a PS homopolymer enables the mixture to microphase-separate, especially for the closed-loop phase transition. On the other hand, the mixtures of PS-*b*-P*n*PMA/PS-06 remain disordered entirely within the experimental temperature range regardless of the amount of PS-06 which corresponds to $\alpha = 0.25$, since this molecular weight is too small to induce the microphase separation. These are harmonious with the prediction by Noolandi and co-worker although it was described for incompressible systems.[5]

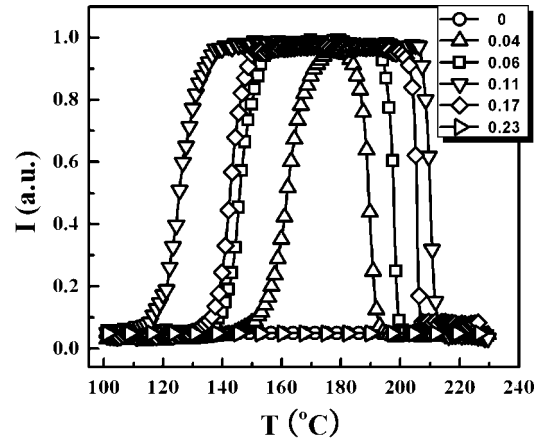

Figure 3. Depolarized light scattering intensity for the mixtures of PS-*b*-P*n*PMA/PS-13 where the amount of PS-13 was varied. This molecular weight of PS-13 corresponds to a chain length ratio (α) of 0.5 with respect to the PS chain length of PS-*b*-P*n*PMA.

SAXS profiles and the scattering parameters for the mixture of PS-*b*-P*n*PMA/PS-13 at $W_{PS\text{-}13} = 0.11$ are shown in Figure 4, measured at a heating rate of 0.5 °C/min from 94 to 240 °C during heating process. As temperature increases, a weak and broad scattering maximum due to the disordered state of BCP intensifies near 125 °C corresponding to a LDOT, then the intensity reaches a maximum and begins to diminish near 205 °C corresponding to a UODT. This is the characteristic of a closed-loop phase transition in the experimental temperature range, hence producing the microphase separation between two transitions. These scattering parameters such as $1/I(q_{max})$, fwhm and *d*-spacing (*d*) are plotted in Figure 4b as a function of inverse temperature, where two discernible changes in the parameters were observed near 125 and 205 °C. These are in good agreement in trends with the previous results.[36] It should

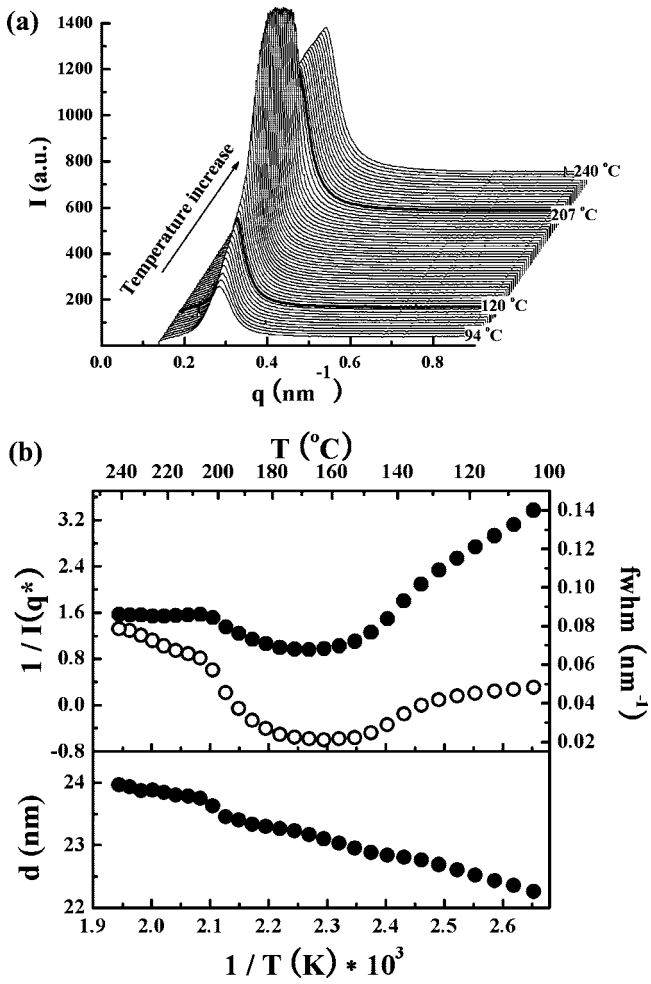

Figure 4. (a) SAXS profiles for the mixture of PS-*b*-P*n*PMA/PS-13 at $W_{PS-13} = 0.11$ measured at a heating rate of 0.5 °C/min^{-1} from 94 to 240 °C. (b) Temperature dependence of the inverse of the maximum intensity ($1/I(q_{max})$; ●), full-width at half-maximum (fwhm; ○), and *d*-spacing (*d*) by $d = 2\pi/q_{max}$. A LDOT and a UODT were obtained by the discernible discontinuity in scattering parameters near 125 and 205 °C, respectively.

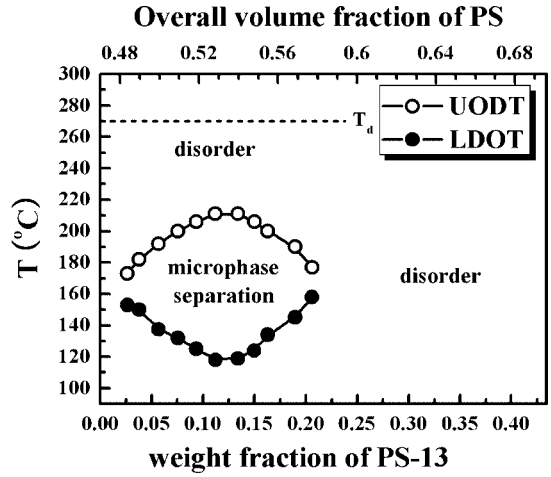

Figure 5. Phase diagram for the mixtures of PS-*b*-P*n*PMA/PS-13 measured by the depolarized light scattering from 110 to 260 °C at a heating rate of 0.5 °C /min. Two transition temperatures such as LDOT and UODT of the closed-loop were obtained from $W_{PS-13} = 0.026$ ($f_{PS} = 0.48$) to $W_{PS-13} = 0.21$ ($f_{PS} = 0.58$), where microphase separation was observed inside of closed-loop.

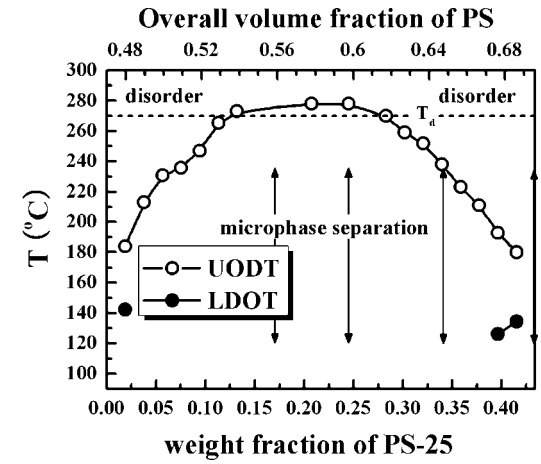

Figure 6. Phase diagram for the mixtures of PS-*b*-P*n*PMA/PS-25, measured by the depolarized light scattering from 110 to 290 °C at a heating rate of 0.5 °C /min. Two transition temperatures such as LDOT and UODT of the closed-loop were obtained at $W_{PS-25} = 0.019$ ($f_{PS} = 0.48$), $W_{PS-25} = 0.40$ ($f_{PS} = 0.68$), and $W_{PS-25} = 0.42$ ($f_{PS} = 0.69$), where microphase separation was observed inside of closed-loop. SAXS measurements for the mixtures were performed at several compositions to support microdomain morphology, indicated by the double headed arrows.

be noted that the difference of two transition temperatures between the depolarized light scattering and SAXS may result from the broad transitions or the different measurement mechanisms within the experimental error range of ± 7 °C.

The transition temperatures for the mixtures of PS-*b*-P*n*PMA/PS-13, measured by the depolarized light scattering, are shown in Figure 5 as a function of W_{PS-13}, leading to a closed-loop type phase diagram as would be expected. From the disordered state for PS-*b*-P*n*PMA as itself, two transition temperatures such as LDOT (153 °C) and UODT (173 °C) of the closed-loop were observed at $W_{PS-13} = 0.026$ ($f_{PS} = 0.48$), with increasing amount of PS-13, followed by the decrease of LDOT and the increase of UODT. Two extreme temperatures correspond to 118 and 211 °C at $W_{PS-13} = 0.11$ ($f_{PS} = 0.53$) as a critical amount for PS-13, and these transitions disappear at $W_{PS-13} = 0.23$ ($f_{PS} = 0.59$). At greater than $W_{PS-13} = 0.23$, consequently it turns out to be disordered for the mixtures of PS-*b*-P*n*PMA/PS-13. By assuming that PS-13 is solubilized in the PS microdomains of PS-*b*-P*n*PMA, the compositional sensitivity to the closed-loop phase behavior possibly provides a rationale for this new window on the closed-loop phase transition induced by PS homopolymers,[44] because the composition of $f_{PS} = 0.465$ for the homopolymer-free PS-*b*-P*n*PMA at disordered regime out of the phase boundary, with increasing amount of PS-13, approaches to a critical composition of $W_{PS-13} = 0.11$ ($f_{PS} =$ 0.53) at ordered state of the closed-loop, which is caused by the greatest increment of the compressibility difference between two components in the mixture as an entropic contribution, and then inversely asymmetric composition at greater than $W_{PS-13} = 0.12$, at which it destabilizes the ordered phase in the weak segregation regime.

Figure 6 shows the phase diagram for the mixtures of PS-*b*-P*n*PMA/PS-25 as a function of W_{PS-25} ($\alpha = 1$), where all the data were measured by the depolarized light scattering in similar way to the prior results. At $W_{PS-25} = 0.019$ ($f_{PS} = 0.48$), adding small amount of PS-25 led to two transition temperatures such as LDOT (142 °C) and UODT (184 °C) of the closed-loop from the disordered state for PS-*b*-P*n*PMA. With further increasing amount of PS-25 up to $W_{PS-25} = 0.38$ ($f_{PS} = 0.67$), only UODT increases to a maximum (278 °C) and decreases, which is in similar tendency to the response of PS-13 in the mixtures although a critical amount of PS-25 (at $W_{PS-25} = 0.21$) is greater than that of PS-13 (at $W_{PS-13} = 0.11$). Whereas for LDOT, all

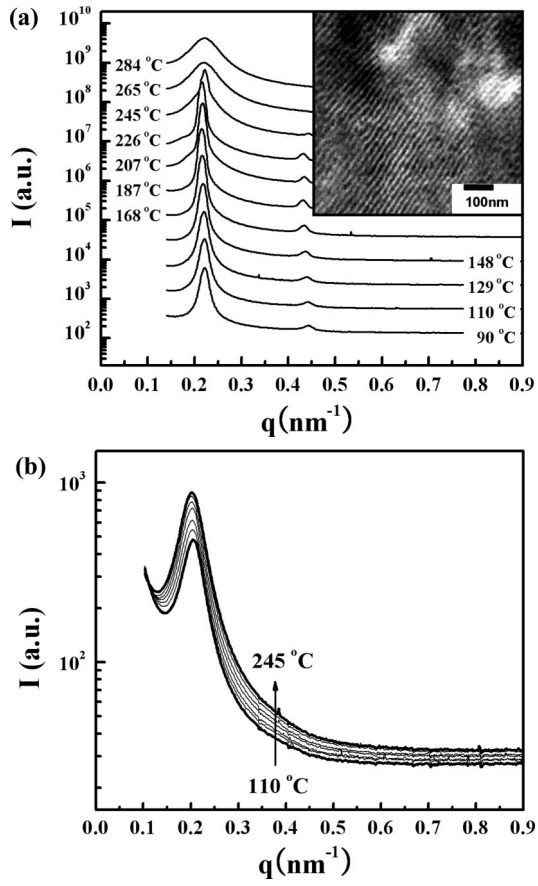

Figure 7. (a) SAXS profiles for the mixture of PS-*b*-P*n*PMA/PS-25 at $W_{PS\text{-}25} = 0.34$ ($f_{PS} = 0.65$), measured at various temperatures from 90 to 284 °C during heating process. For clarity, each profile was vertically shifted by a factor of 2.6. TEM image for this mixture was taken after quenching from 180 °C, where PS component was selectively stained with RuO_4. (b) SAXS profiles for the mixture of PS-*b*-P*n*PMA/PS-25 at $W_{PS\text{-}25} = 0.43$ ($f_{PS} = 0.70$), measured at various temperatures from 110 to 245 °C during heating process. A weak and broad maximum due to the correlation hole scattering indicates the entirely disordered state for this mixture within the experimental temperature range.

data were not detectable possibly because it is lower than the glass transition temperature ($T_g \sim 100$ °C) of PS. However, LDOT and UODT of the closed-loop appear at $W_{PS\text{-}25} = 0.40$ ($f_{PS} = 0.68$) and $W_{PS\text{-}25} = 0.42$ ($f_{PS} = 0.69$), and these transitions disappear at greater than $W_{PS\text{-}25} = 0.43$ ($W_{PS} = 0.70$).

SAXS experiments were performed to support the results of the depolarized light scattering for the mixtures of PS-*b*-P*n*PMA/PS-25 at $W_{PS\text{-}25} = 0.17$, 0.25, 0.34, and 0.43, as marked by double headed arrows in Figure 6. Figure 7a shows SAXS profiles for the mixture of PS-*b*-P*n*PMA/PS-25 at $W_{PS\text{-}25} = 0.34$ ($f_{PS} = 0.65$), measured at approximately 20 °C intervals from 90 to 284 °C during heating process. Within ordered range at lower than 240 °C, measured by the depolarized light scattering in Figure 6, a sharp scattering intensity and second-order peak are seen at scattering vector ratios of 1:2 relative to a primary peak since this mixture microphase-separates into a lamellar morphology as evidenced in transmission electron microscopy (TEM). At higher than 245 °C which corresponds to a UODT, the primary peak weakens and broadens abruptly and the second-order peak disappears, resulting in a weak and diffuse maximum due to the disordered state of BCP. It should be mentioned that thermal degradation temperature (T_d) was set to 270 °C in this study even though some data were taken above T_d for more information. Figure 7b shows SAXS profiles for the mixture of PS-*b*-P*n*PMA/PS-25 at $W_{PS\text{-}25} = 0.43$ ($f_{PS} = 0.70$) during heating process. At all temperatures measured up to 245 °C, a weak and broad scattering maximum with no higher-order peak was observed, confirming the entirely disordered state within the experimental temperature range as is the case of the homopolymer-free PS-*b*-P*n*PMA in Figure 2.

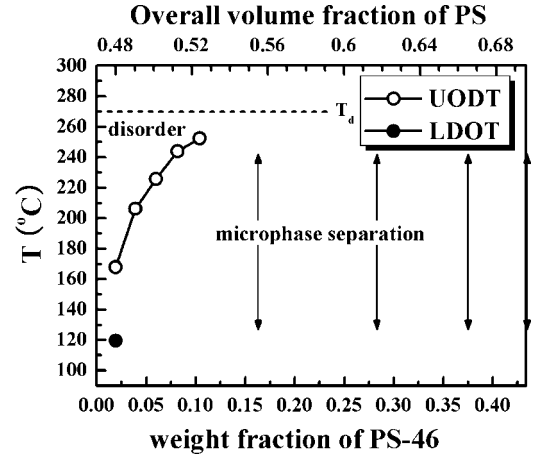

Figure 8. Phase diagram for the mixtures of PS-*b*-P*n*PMA/PS-46, measured by the depolarized light scattering from 110 to 290 °C at a heating rate of 0.5 °C /min. Two transition temperatures such as LDOT and UODT of the closed-loop were obtained only at $W_{PS\text{-}25} = 0.019$ ($f_{PS} = 0.48$). SAXS measurements for the mixtures were performed at several compositions to support microdomain morphology, indicated by the double headed arrows.

For $\alpha = 2$, the phase diagram for the mixtures of PS-*b*-P*n*PMA/PS-46 is shown in Figure 8. Only at $W_{PS\text{-}46} = 0.019$ ($f_{PS} = 0.48$), adding small amount of PS-46 allows two transition temperatures such as LDOT (120 °C) and UODT (168 °C) of the closed-loop from the disordered state for PS-*b*-P*n*PMA. With further increasing amount of PS-46, only UODT increases and LDOT disappears, indicating the ordered state at greater than $W_{PS\text{-}46} = 0.10$ ($f_{PS} = 0.52$). Consequently, the increased molecular weight of PS in the mixture of PS-*b*-P*n*PMA/PS has influence on the transition temperatures remarkably leading to the extended closed-loop phase boundary. A similar molecular weight dependence of homopolymers on the LDOT was observed for the mixtures of PS-*b*-P*n*BMA/PS,[32] which can be attributed to the fact that with increasing molecular weight of PS, the loss of the combinatorial entropy becomes significant due to the dominant localization of PS. It should be also pointed out that no macrophase separation occurs for the mixtures up to the largest amount of PS ($W_{PS} = 0.43$ or $f_{PS} = 0.70$) regardless of molecular weight of PS in this study.

Figure 9 shows SAXS profiles measured at various temperatures during heating process and TEM images for the mixtures of PS-*b*-P*n*PMA/PS-46. All profiles with corresponding temperatures indicate a sharp scattering intensity and second-order peak at scattering vector ratios of 1:2 relative to a primary peak for these mixtures at $W_{PS\text{-}46} = 0.28$ ($f_{PS} = 0.62$) and $W_{PS\text{-}46} = 0.43$ ($f_{PS} = 0.70$) in Figure 9, parts a and b, respectively, with the consistent lamellar morphologies over the entire temperature range in insets.

Here, the phase stability of the closed-loop phase behavior should be discussed since the morphology persists in a lamellar microdomain even up to $W_{PS\text{-}46} = 0.43$ ($f_{PS} = 0.70$) for the mixture of PS-*b*-P*n*PMA/PS-46. To elucidate the phase stability for the mixtures of PS-*b*-P*n*PMA/PS, let us turn our attention to the solubilization of PS homopolymers having chain length ratios of $\alpha = 0.5$, 1, and 2. It was reported by Hashimoto et al. that the change of *d*-spacing by homopolymer estimates whether the solubilization behavior of homopolymers is uniform or localized in the mixtures of BCP/homopolymer, which is in turn related to the phase stability.[13,15,16] The uniform solubilization

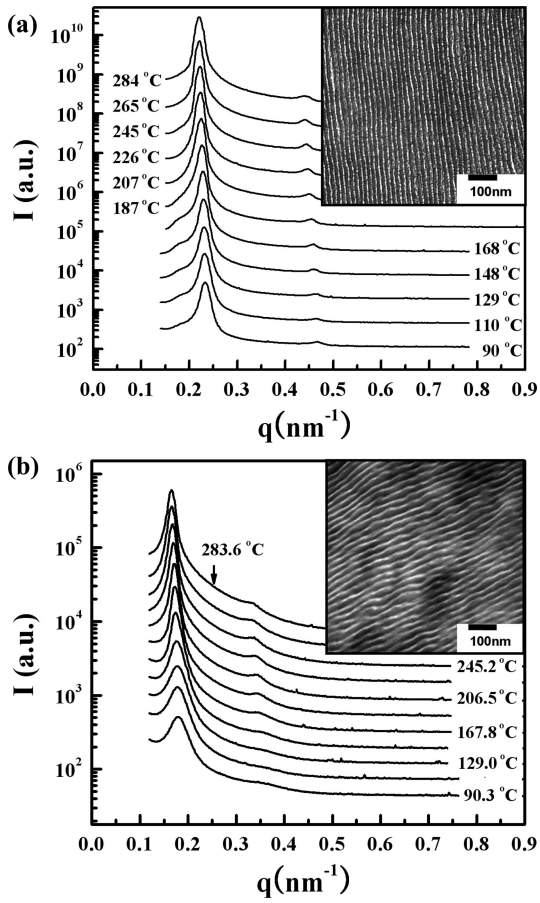

Figure 9. SAXS profiles measured at various temperatures from 90 to 284 °C during heating process and TEM images taken after quenching from 180 °C for the mixture of PS-*b*-P*n*PMA/PS-46 at (a) $W_{PS\text{-}46} = 0.28$ ($f_{PS} = 0.62$) and (b) $W_{PS\text{-}46} = 0.43$ ($f_{PS} = 0.70$). For clarity, each SAXS profile was vertically shifted by a factor of 3 and 1.5, respectively.

of homopolymer involves a swollen microdomain and the contraction of the other microdomain, caused by an expansion of the average distances between the chemical junctions. In contrast, the localized solubilization by homopolymer involves only expanded microdomain normal to the interfaces due to the localized homopolymer in the middle of microdomains and no contraction of the other microdomain, leading to the same average distances between the chemical junctions.[13]

From the volumetric consideration for the lamellar microdomain of the mixtures, the expansion ratio of *d*-spacing can be correlated to the change of the interfacial density of the chemical junctions as given by

$$d/d_o = \frac{\rho_J}{\rho_{Jo} f_B} = \frac{\rho_J}{\rho_{Jo}(1 - f_{HPS})} \quad (1)$$

where d, d_o are *d*-spacings, ρ_J, ρ_{Jo} are the interfacial densities of the chemical junctions after and before adding PS homopolymers, and f_B, f_{HPS} are the volume fraction of PS-*b*-P*n*PMA and PS homopolymers added in this study, respectively. An extreme condition, $\rho_J/\rho_{Jo} = 1$, can be assumed in the case of the localized solubilization of PS, by yielding d/d_o as a simple relation to volume fraction of PS homopolymers.[15] Figure 10a shows *d*-spacing (or interlamellar spacing) and the expansion ratios of *d*-spacing taken from SAXS profiles at 180 °C as a function of weight fraction of PS homopolymers (W_{HPS}) for the mixtures of PS-*b*-P*n*PMA/PS, in which the solid line indicates the localized solubilization of PS by the condition of $\rho_J/\rho_{Jo} = 1$ and $d_o = 22.0$ nm. The *d*-spacings (or the expansion ratios of

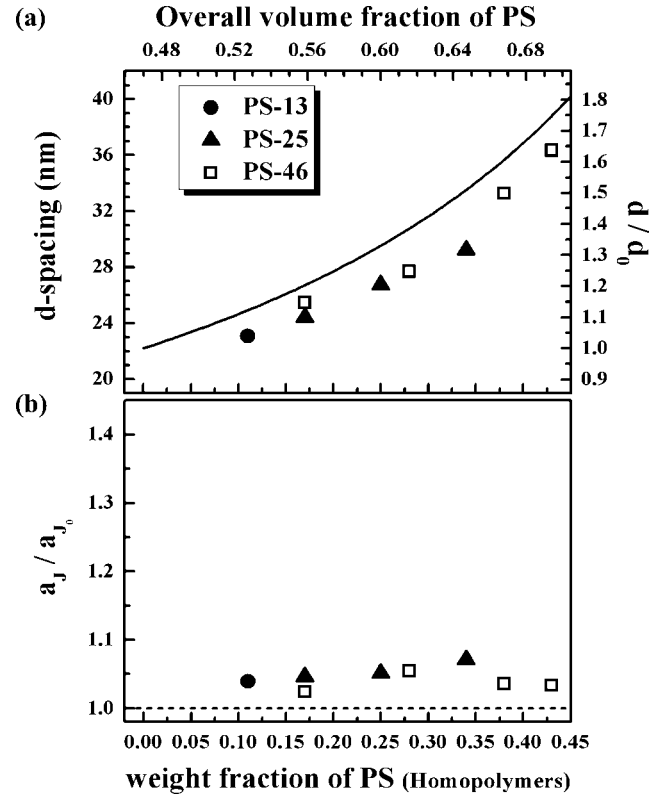

Figure 10. (a) *d*-spacing (or interlamellar spacing; left), the expansion ratio of *d*-spacing (right), and (b) the expansion ratio of a_J/a_{Jo} taken from SAXS profiles at 180 °C for the mixtures of PS-*b*-P*n*PMA/PS, in which the solid line indicates the localized solubilization of PS by the condition of $\rho_J/\rho_{Jo} = 1$ and $d_o = 22.0$ nm by $d = 2\pi/q_{max}$.

d-spacing) increase with increasing amount of PS, which are placed close to the solid line. These data predict the dominant localized PS homopolymer chains which tend to be segregated in the middle of microdomain layers for the mixtures of PS-*b*-P*n*PMA/PS, rather than the uniform solubilization of PS homopolymer. Alternative simple equation between the interfacial densities (ρ_J, ρ_{Jo}) of the chemical junctions and the average distances (a_J, a_{Jo}) between the chemical junctions after and before adding PS homopolymers is given by

$$\frac{a_J}{a_{Jo}} \cong \left[\frac{\rho_J}{\rho_{Jo}}\right]^{-1/2} \quad (2)$$

where a_J, a_{Jo} are the average nearest-neighbor distances between the chemical junctions along the interfaces after and before adding PS homopolymers.[15] Figure 10b displays the expansion ratio of a_J/a_{Jo} as a function of W_{HPS}. From the data closer to $a_J/a_{Jo} = 1$, it confirms that the localization model in this system is valid for $\alpha = 0.5$, 1, and 2 although minor in deviations, resulting in the conservation of lamellar morphology, possibly because a_J is little influenced by the localized solubilization of PS and only the thickness of PS microdomains increases with little effect to the other P*n*PMA microdomains.

In summary, the closed-loop phase transition induced by homopolymers was investigated in the mixtures of PS-*b*-P*n*PMA/PS in the weak segregation regime from the disordered state of homopolymer-free PS-*b*-P*n*PMA. For the binary mixtures with low molecular weight of PS ($\alpha \ll 0.5$), they remain disordered within the experimental temperature range, whereas for the mixtures with higher molecular weight of PS ($\alpha = 0.5$, 1, and 2), both LDOT and UODT of the closed-loop were obtained and the transition temperature dependence on composition was appreciable where a critical amount of PS of the closed-loop transition increased from $W_{PS\text{-}13} = 0.11$ to $W_{PS\text{-}25} = 0.21$

and greater value of $W_{PS\text{-}46}$, leading to the extended phase boundary of the closed-loop as is the case of $\alpha = 2$. From the *d*-spacing (or interlamellar spacing) and expansion ratio of a_J/a_{Jo}, the phase stability of the mixtures indicates that PS chains (in case of $\alpha = 0.5$, 1, and 2) are dominantly localized in the middle of PS microdomains, allowing the conservation of lamellar morphology up to the overall PS volume fraction of 0.70 in the case of $\alpha = 2$.

Acknowledgment. This work was supported by the Nuclear R&D Programs and APCPI ERC program (R11-2007-050-01004) funded by the Ministry of Education, Science & Technology (MEST), Seoul Research and Business Development Program (10816 ICBIN), Korea. J. K. K. acknowledges the National Creative Research Initiative Program supported by the Korea Science and Engineering Foundation (KOSEF), and T. C. also acknowledges the National Research Laboratory Program (R0A-2007-000-20125-0) supported by the KOSEF.

References and Notes

(1) Rigby, D.; Roe, R. J. *Macromolecules* **1984**, *17*, 1778–1785.
(2) Roe, R. J.; Zin, W. C. *Macromolecules* **1984**, *17*, 189–194.
(3) Zin, W. C.; Roe, R. J. *Macromolecules* **1984**, *17*, 183–188.
(4) Rigby, D.; Lin, J. L.; Roe, R. J. *Macromolecules* **1985**, *18*, 2269–2273.
(5) Whitmore, M. D.; Noolandi, J. *Macromolecules* **1985**, *18*, 2486–2497.
(6) Rigby, D.; Roe, R. J. *Macromolecules* **1986**, *19*, 721–728.
(7) Roe, R. J. *Macromolecules* **1986**, *19*, 728–731.
(8) Olvera de la Cruz, M.; Sanchez, I. C. *Macromolecules* **1987**, *20*, 440–443.
(9) Nojima, S.; Roe, R. J. *Macromolecules* **1987**, *20*, 1866–1876.
(10) Kinning, D. J.; Winey, K. I.; Thomas, E. L. *Macromolecules* **1988**, *21*, 3502–3506.
(11) David, J. K.; Edwin, L. T.; Lewis, J. F. *J. Chem. Phys.* **1989**, *90*, 5806–5825.
(12) Owens, J. N.; Gancarz, I. S.; Koberstein, J. T.; Russell, T. P. *Macromolecules* **1989**, *22*, 3388–3394.
(13) Hashimoto, T.; Tanaka, H.; Hasegawa, H. *Macromolecules* **1990**, *23*, 4378–4386.
(14) Karen, I. W.; Edwin, L. T.; Lewis, J. F. *J. Chem. Phys.* **1991**, *95*, 9367–9375.
(15) Tanaka, H.; Hasegawa, H.; Hashimoto, T. *Macromolecules* **1991**, *24*, 240–251.
(16) Tanaka, H.; Hashimoto, T. *Macromolecules* **1991**, *24*, 5713–5720.
(17) Kang, C. K.; Zin, W. C. *Macromolecules* **1992**, *25*, 3039–3045.
(18) Hashimoto, T.; Koizumi, S.; Hasegawa, H.; Izumitani, T.; Hyde, S. T. *Macromolecules* **1992**, *25*, 1433–1439.
(19) Winey, K. I.; Thomas, E. L.; Fetters, L. J. *Macromolecules* **1992**, *25*, 2645–2650.
(20) Disko, M. M.; Liang, K. S.; Behal, S. K.; Roe, R. J.; Jeon, K. J. *Macromolecules* **1993**, *26*, 2983–2986.
(21) Hashimoto, T.; Yamasaki, K.; Koizumi, S.; Hasegawa, H. *Macromolecules* **1993**, *26*, 2895–2904.
(22) Pan, T.; Huang, K.; Balazs, A. C.; Kunz, M. S.; Mayes, A. M.; Russell, T. P. *Macromolecules* **1993**, *26*, 2860–2865.
(23) Spontak, R. J.; Smith, S. D.; Ashraf, A. *Macromolecules* **1993**, *26*, 956–962.
(24) Spontak, R. J.; Smith, S. D.; Ashraf, A. *Macromolecules* **1993**, *26*, 5118–5124.
(25) Jeon, K.-J.; Roe, R.-J. *Macromolecules* **1994**, *27*, 2439–2447.
(26) Koizumi, S.; Hasegawa, H.; Hashimoto, T. *Macromolecules* **1994**, *27*, 6532–6540.
(27) Koizumi, S.; Hasegawa, H.; Hashimoto, T. *Macromolecules* **1994**, *27*, 7893–7906.
(28) Loewenhaupt, B.; Steurer, A.; Hellmann, G. P.; Gallot, Y. *Macromolecules* **1994**, *27*, 908–916.
(29) Matsen, M. W. *Macromolecules* **1995**, *28*, 5765–5773.
(30) Janert, P. K.; Schick, M. *Macromolecules* **1998**, *31*, 1109–1113.
(31) Lee, J. H.; Balsara, N. P.; Chakraborty, A. K.; Krishnamoorti, R.; Hammouda, B. *Macromolecules* **2002**, *35*, 7748–7757.
(32) Kim, E. Y.; Lee, D. J.; Kim, J. K.; Cho, J. *Macromolecules* **2006**, *39*, 8747–8757.
(33) Kim, J. K.; Lee, J. I.; Lee, D. H. *Macromol. Res.* **2008**, *16*, 267–292.
(34) Russell, T. P.; Karis, T. E.; Gallot, Y.; Mayes, A. M. *Nature (London)* **1994**, *368*, 729–731.
(35) Ruzette, A. V. G.; Banerjee, P.; Mayes, A. M.; Pollard, M.; Russell, T. P.; Jerome, R.; Slawecki, T.; Hjelm, R.; Thiyagarajan, P. *Macromolecules* **1998**, *31*, 8509–8516.
(36) Ryu, D. Y.; Jeong, U.; Kim, J. K.; Russell, T. R. *Nat. Mater. (London)* **2002**, *1*, 114–117.
(37) Ryu, D. Y.; Jeong, U.; Lee, D. H.; Kim, J.; Youn, H. S.; Kim, J. K. *Macromolecules* **2003**, *36*, 2894–2902.
(38) Ryu, D. Y.; Lee, D. J.; Kim, J. K.; Lavery, K. A.; Russell, T. P.; Han, Y. S.; Seong, B. S.; Lee, C. H.; Thiyagarajan, P. *Phys. Rev. Lett.* **2003**, *90*, 235501.
(39) Ryu, D. Y.; Lee, D. H.; Jang, J.; Kim, J. K.; Lavery, K. A.; Russell, T. P. *Macromolecules* **2004**, *37*, 5851–5855.
(40) Ryu, D. Y.; Lee, D. H.; Jeong, U.; Yun, S. H.; Park, S.; Kwon, K.; Sohn, B. H.; Chang, T.; Kim, J. K.; Russell, T. P. *Macromolecules* **2004**, *37*, 3717–3724.
(41) Kim, H. J.; Kim, S. B.; Kim, J. K.; Jung, Y. M. *J. Phys. Chem. B* **2006**, *110*, 23123–23129.
(42) Kim, H. J.; Kim, S. B.; Kim, J. K.; Jung, Y. M.; Ryu, D. Y.; Lavery, K. A.; Russell, T. P. *Macromolecules* **2006**, *39*, 408–412.
(43) Ryu, D. Y.; Shin, C.; Cho, J.; Lee, D. H.; Kim, J. K.; Lavery, K. A.; Russell, T. P. *Macromolecules* **2007**, *40*, 7644–7655.
(44) Hwang, S. W.; Kim, E.; Shin, C.; Kim, J. H.; Ryu, D. Y.; Park, S.; Chang, T.; Kim, J. K. *Macromolecules* **2007**, *40*, 8066–8070.
(45) Cho, J. *Macromolecules* **2004**, *37*, 10101–10108.
(46) Park, S.; Cho, D.; Ryu, J.; Kwon, K.; Chang, T.; Park, J. *J. Chromatogr. A* **2002**, *958*, 183–189.
(47) Leibler, L. *Macromolecules* **1980**, *13*, 1602–1617.

MA801530F